

# Lawrence Berkeley National Laboratory

## LBL Publications

**Title**

EFFECTS OF GAMMA-IRRADIATION ON ACTINIDE IONS IN CALCIUM FLUORIDE

**Permalink**

<https://escholarship.org/uc/item/9s11z82p>

**Author**

Stacy, J.J.

**Publication Date**

1972-03-01

EFFECTS OF GAMMA-IRRADIATION ON ACTINIDE  
IONS IN CALCIUM FLUORIDE

J. J. Stacy, N. Edelstein, and R. D. McLaughlin

March 1972

AEC Contract No. W-7405-eng-48

TWO-WEEK LOAN COPY

This is a Library Circulating Copy  
which may be borrowed for two weeks.  
For a personal retention copy, call  
Tech. Info. Division, Ext. 5545



4

## **DISCLAIMER**

This document was prepared as an account of work sponsored by the United States Government. While this document is believed to contain correct information, neither the United States Government nor any agency thereof, nor the Regents of the University of California, nor any of their employees, makes any warranty, express or implied, or assumes any legal responsibility for the accuracy, completeness, or usefulness of any information, apparatus, product, or process disclosed, or represents that its use would not infringe privately owned rights. Reference herein to any specific commercial product, process, or service by its trade name, trademark, manufacturer, or otherwise, does not necessarily constitute or imply its endorsement, recommendation, or favoring by the United States Government or any agency thereof, or the Regents of the University of California. The views and opinions of authors expressed herein do not necessarily state or reflect those of the United States Government or any agency thereof or the Regents of the University of California.

EFFECTS OF GAMMA-IRRADIATION ON ACTINIDE IONS IN CALCIUM FLUORIDE<sup>†</sup>

J. J. Stacy, N. Edelstein, and R. D. McLaughlin

Lawrence Berkeley Laboratory  
University of California  
Berkeley, California 94720

March 1972

ABSTRACT

Optical absorption and thermoluminescence measurements were used to study the effects of gamma-irradiation on trivalent actinide ions in  $\text{CaF}_2$ . Thermoluminescent glow curves for Np, Pu, Am and Cm (and, for comparison, the lanthanides Er, Ho and Tm) were measured between 100° and 300°K. These were found to be remarkable similar, with glow peaks occurring at nearly the same temperatures for each of the ions. High resolution measurements of the spectra of the thermoluminescence showed that the emission is similar to the fluorescence of the trivalent ions. Evidence is presented that the glow emission below 300°K originates from trivalent actinide ions in cubic sites. When the actinide- $\text{CaF}_2$  crystals were irradiated at 300°K, the actinide ion was oxidized to the tetravalent state. A mechanism has been proposed to explain these observations.

INTRODUCTION

Small amounts of lanthanide ions incorporated in crystals of  $\text{CaF}_2$  exhibit the optical spectra of the trivalent state. However the main feature is the appearance of many absorption (or emission) lines from multiple symmetry sites due to different types of charge compensation of the tripositive ion in a dipositive host crystal.<sup>1</sup> The main feature of chemical interest is that the

dipositive state of the entire lanthanide series may be produced and stabilized in  $\text{CaF}_2$  by three methods: gamma irradiation<sup>2</sup>; electrolytic reduction<sup>3</sup>; or baking in calcium vapor.<sup>4</sup> The last two techniques are performed at elevated temperatures and result in a thermally stable divalent lanthanide ion in much higher concentrations than obtained with the first method.

Merz and Pershan<sup>5</sup> (from now on called MP) have performed a detailed study of the effects of x-ray or gamma ray irradiation on the trivalent lanthanide ions in  $\text{CaF}_2$  crystals. Their conclusions may be summarized as follows: 1) lanthanide ions in cubic symmetry sites are reduced to the divalent state by irradiation; 2) subsequent heating of these crystals causes the oxidation of the divalent ion with a characteristic emission of light from the trivalent ion; 3) the temperatures at which the thermoluminescence occurs does not depend on the particular lanthanide ion; and 4) the characteristic luminescence from the trivalent ions below room temperature is only from these ions in cubic sites; above room temperature the luminescence occurs from ions in tetragonal sites. On the basis of the above experimental observations MP proposed a model to explain the reduction-oxidation-thermoluminescence processes in these crystals.

Actinide ions incorporated in  $\text{CaF}_2$  crystals have been the subject of a number of studies in our laboratory.<sup>6-9</sup> Two of these ions,  $\text{Am}^{3+}$  and  $\text{Es}^{3+}$ , behave similarly to the lanthanide ions in that irradiation causes the formation of the dipositive ions as shown by electron paramagnetic resonance (epr) investigations. However in the cases of the  $\text{Np}^{3+}$ ,  $\text{Pu}^{3+}$ , and  $\text{Cm}^{3+}$ , irradiation caused the oxidation of these ions to the tetrapositive state. In this paper we report the results of our optical investigations on actinide ions in  $\text{CaF}_2$  crystals.

### EXPERIMENTAL

Actinide ions doped in  $\text{CaF}_2$  crystals were prepared in the same manner as discussed previously.<sup>10</sup> The actinide ions in concentrated acid solution were added to powdered  $\text{CaF}_2$  containing 2 wt.%  $\text{PbF}_2$ , which was used as a scavenger for water and oxygen. Other samples containing lanthanide ions or uranium ions were purchased from Optovac, Inc.<sup>11</sup> The concentration of the dopant ion in the crystal was not determined. The initial doping levels before crystal growth varied from 0.01-0.8 wt.%; however, the amount retained in the crystal after melting can vary widely from this figure.

Spectral measurements were made photographically using a Jarrell-Ash F/6.3 plane grating spectrograph which had, in the first order, a reciprocal linear dispersion of approximately  $10\text{\AA}/\text{mm}$  at the blaze wavelength,  $5000\text{\AA}$ . A Cary Model 14 recording spectrometer was used in the infrared region. Quantitative absorption measurements were made with a Jarrell-Ash Model 82-000 0.5 meter Ebert scanning spectrometer used with an RCA 7102 photomultiplier which was cooled by a flow of cold nitrogen gas.

Single crystals of  $\text{CaF}_2$  containing various impurity ions were exposed to gamma rays from a  $^{60}\text{Co}$  source of approximately  $6 \times 10^6$  roentgens/min. for various lengths of time. The temperature at which this irradiation took place could be changed by placing the sample in a small dewar containing either liquid nitrogen or an ice-water bath.

Glow curves were obtained by slowly warming the crystals from  $\sim 100^\circ\text{K}$  to room temperature by means of an adjustable flow of cold nitrogen gas. The temperature was measured with a resistance thermometer which gave a linear response in the temperature range  $100^\circ\text{K}$ - $300^\circ\text{K}$  and was calibrated with a

chromel-alumel thermocouple. Temperature measurements were accurate to  $\pm 2^\circ\text{K}$  and precise to  $0.5^\circ\text{K}$ . The glow intensity was integrated over wavelength according to the S-20 spectral response of the photomultiplier and plotted as a function of temperature. The heating rate was not linear and varied from  $0.5^\circ/\text{minute}$  at the beginning of a run to  $5.0^\circ/\text{minute}$  at the end of the run. Thermoluminescence measurements above room temperature were obtained by heating the crystal with a resistance coil and measuring the temperature with a chromel-alumel thermocouple.

## RESULTS

### SHARP LINE SPECTRA

#### A. NEPTUNIUM

Single crystals of  $\text{CaF}_2$  doped with 0.1-0.2 wt.%  $^{237}\text{Np}$  were light green in color. A comparison of the absorption spectrum of these crystals with data on  $\text{Np}^{3+}$  in  $\text{LaBr}_3$  and solution data of several oxidation states<sup>12,13</sup> of  $\text{Np}$  is shown in Fig. 1. The main oxidation state present in the  $\text{CaF}_2$  crystals is  $\text{Np}^{3+}$  without any significant amount of  $\text{Np}^{4+}$  or  $\text{Np}^{6+}$ . The presence of  $\text{Np}^{5+}$  cannot be rigorously excluded since its only intense peak overlaps with an  $\text{Np}^{3+}$  peak but from the conditions of crystal growth its formation is not very probable and we exclude its presence.

When the  $\text{Np}^{3+}\text{-CaF}_2$  crystal was irradiated for 15 hours at  $0^\circ\text{C}$  or at room temperature in the  $^{60}\text{Co}$  source it turned to a deep blue-green color. An intense broad absorption appeared in the visible region (discussed later) and also three new groups of sharp lines. By comparison with the most intense absorptions of  $\text{Np}^{4+}$  in  $\text{D}_2\text{O}^{13}$  (Fig. 1) and various other  $\text{Np}^{4+}$  spectra<sup>14</sup> these lines were assigned to  $\text{Np}^{4+}$ . The radiation induced  $\text{Np}^{4+}$  was not completely stable and decreased slightly in intensity over a period of a few months at room temperature. The broad absorption band and the  $\text{Np}^{4+}$  structure could be

bleached out by heating the crystal to  $\sim 400^\circ\text{C}$ . A one hour exposure with 3000-5000 $\text{\AA}$  radiation from a 1000 watt Hg lamp reduced the intensity of the broad absorption by more than 50%. Additional exposure seemed to have little effect.

A high resolution quantitative study was made of the growth of  $\text{Np}^{4+}$  and the decay of  $\text{Np}^{3+}$  spectral lines upon gamma irradiation at  $0^\circ\text{C}$ . Because of the relatively poor sensitivity of the PbS detector, measurements above  $1\mu$  in wavelength could not easily be made so only the spectral region between 9400-10000 $\text{\AA}$  was intensively studied. The absorption spectrum of  $\text{Np-CaF}_2$  before and after irradiation is shown in Fig. 2. Twelve  $\text{Np}^{3+}$  lines could be followed; eight remained unchanged and four decreased in intensity. In addition four new sharp lines appeared which were assigned to  $\text{Np}^{4+}$  for the following reasons. These new lines at  $\sim 9500\text{\AA}$  appeared under the same conditions as the  $\text{Np}^{4+}$  lines at  $1.7\mu$  which could only be assigned to this oxidation state. If this new structure was due to site symmetry changes of  $\text{Np}^{3+}$  then in each absorption region of  $\text{Np}^{3+}$  one would expect to find new lines. In the  $\text{Np}^{3+}$  region at  $2.3\mu$  no new lines appeared so this possibility was excluded.

The growth and decay of various lines between 9400-10000 $\text{\AA}$  as a function of irradiation time is shown in Fig. 3. The height of the absorption band was assumed to be proportional to the concentration of ions, since the linewidth did not change upon irradiation. In Fig. 4 the relative change in the optical density of  $\text{Np}^{3+}$  is plotted vs. the relative change in the optical density of  $\text{Np}^{4+}$  for the two strongest sets of lines. The slope of the line through the points was  $\sim 1$ . From this fact we conclude the growth of the  $\text{Np}^{4+}$  lines was correlated with the decay of the  $\text{Np}^{3+}$  lines and the equation<sup>15</sup>



$$\frac{OD_{Np^{3+}} - OD_{Np^{3+}}(t=0)}{OD_{Np^{3+}}(t=0) - OD_{Np^{3+}}(t=\infty)} = \frac{OD_{Np^{4+}} - OD_{Np^{4+}}(t=0)}{OD_{Np^{4+}}(t=0) - OD_{Np^{4+}}(t=\infty)} \quad (1)$$

was followed, where the additional subscripts  $t=0$  and  $t=\infty$  represent, respectively, the optical densities of the initial (unirradiated) state and the state irradiated to saturation. Further analysis of the data in Fig. 3 showed that the rate of decay of  $Np^{3+}$  is not first order. The oxidation of  $Np^{3+}$ , therefore, is not by direct irradiation but occurs via a more complex mechanism. Complete wavelength measurements could only be made for the  $Np^{4+}$  lines in the wavelength region of  $1.7\mu$ . In the other regions overlapping lines from the  $Np^{3+}$  ions interfered. The number of levels found for the  $Np^{4+}$  formed by room temperature irradiation was eight. This manifold was assigned a J-value of  $11/2$  by analogy to assignments made in other  $Np^{4+}$  compounds. For absorption spectra from only the ground crystal field level a maximum of six lines can be attained from one symmetry site. If we assume more than one lower level contributes to the absorption lines at  $77^\circ K$ , we should observe some constant differences between the observed lines. Calculation of all possible energy differences showed no constant differences to within experimental error so we conclude the absorption lines at  $1.7\mu$  are due to at least two different  $Np^{4+}$  symmetry sites.

The above result was confirmed by gamma irradiation of the  $Np^{3+}-CaF_2$  crystal at  $77^\circ K$  for 48 hours where only two  $Np^{4+}$  lines appeared in the  $1.7\mu$  region. This excludes the possibility that the surplus lines are due to vibronic transitions. These lines were also present (at twice the intensity) in the  $0^\circ C$  irradiation. The most pronounced effect of the irradiation at  $77^\circ K$ , however, is the spectral changes in the  $Np^{3+}$  region of the infrared. Between  $1.9$  and  $2.4\mu$  three lines appeared, one line originally present increased greatly

in intensity, two lines decreased in intensity and 20 lines were unaffected. Part of this spectral region is shown in Fig. 5. Warming the crystal to room temperature partially bleached the new structure and heating to  $\sim 400^\circ\text{C}$  bleached it completely. It should be emphasized that these  $\text{Np}^{3+}$  changes only occurred for gamma irradiations at  $77^\circ\text{K}$ , not at room temperature. Therefore the mechanism for these site symmetry changes for  $\text{Np}^{3+}$  must be different from that which caused the oxidation of  $\text{Np}^{3+}$  at  $0^\circ\text{C}$ .

#### B. PLUTONIUM

The optical spectrum of Pu in  $\text{CaF}_2$  has been reported previously.<sup>7</sup> Self-irradiation of a  $^{238}\text{Pu-CaF}_2$  crystal at room temperature which originally contained  $\text{Pu}^{3+}$  resulted in the appearance of a new sharp line spectrum which was assigned to  $\text{Pu}^{3+}$  and several broad absorptions assigned to color centers. Self-irradiation of this crystal at  $77^\circ\text{K}$  showed only the formation of the broad absorption bands.

In the present work a  $^{239}\text{Pu-CaF}_2$  crystal containing approximately 0.7 wt.% Pu was irradiated for 48 hours at room temperature in the  $^{60}\text{Co}$  source. Seven sharp lines characteristic of  $\text{Pu}^{4+}$  appeared between 1.83 and  $1.89\mu$ . This crystal was bleached by heating to  $\sim 400^\circ\text{C}$  and then irradiated for 48 hours at  $77^\circ\text{K}$ . Two sharp  $\text{Pu}^{4+}$  lines were observed at 1.836 and  $1.843\mu$  with intensities approximately half of those observed from the room temperature irradiation. A more detailed analysis was not possible because of the weak absorption observed. In fact the detection of  $\text{Pu}^{4+}$  at  $77^\circ\text{K}$  was only possible in a very concentrated crystal at a high radiation dosage.

### C. AMERICIUM

The optical and electron paramagnetic resonance spectra of Am-CaF<sub>2</sub> were reported earlier.<sup>6</sup> Self-irradiation of a <sup>241</sup>Am or <sup>243</sup>Am-CaF<sub>2</sub> crystal results in the formation of Am<sup>2+</sup> in a fashion similar to the lanthanide series. Attempts to find sharp line spectra attributable to Am<sup>4+</sup> at high radiation dosages were unsuccessful.

### D. CURIUM

Preliminary results of the optical spectra of Cm in CaF<sub>2</sub> have been reported.<sup>8</sup> Crystals of CaF<sub>2</sub> doped with <sup>244</sup>Cm (t<sub>1/2</sub>=18 years) are initially colorless but rapidly turn red and eventually black due to self-irradiation damage. A characteristic orange glow at approximately 6000Å due to the <sup>6</sup>P<sub>7/2</sub> → <sup>8</sup>S<sub>7/2</sub> transition of Cm<sup>3+</sup> is always present. Initially only the Cm<sup>3+</sup> ion is present but sharp lines from Cm<sup>4+</sup> rapidly appear. Fewer lines of Cm<sup>4+</sup> appear on irradiation at 77°K. A very intense broad band also appears which obscures the weak Cm<sup>3+</sup> and Cm<sup>4+</sup> absorptions so further analysis was not attempted.

### E. URANIUM

The optical spectrum of U in CaF<sub>2</sub> has been the subject of many conflicting reports. Hargreaves<sup>14</sup> has grown green, red, and yellow crystals of U-CaF<sub>2</sub> which he attributes to U<sup>2+</sup>, U<sup>3+</sup>, and U<sup>4+</sup> respectively. McLaughlin et al.<sup>15</sup> have performed chemical analyses on similar crystals and attribute the spectra from the green crystal to U<sup>4+</sup>, the yellow crystal to U<sup>6+</sup>, and the red crystal to U<sup>3+</sup>.

A very concentrated red crystal was used for the present work. The optical spectrum before gamma irradiation contained spectral lines in the

1.50-1.65 $\mu$  region attributable to the green U species. Irradiation at room temperature for 64 hours doubled the intensity of these lines. Since the chemical properties of U are very similar to those of Np we assign these lines to U<sup>4+</sup>.

#### BROAD ABSORPTION SPECTRA

Another characteristic of the actinide - CaF<sub>2</sub> systems upon gamma or alpha irradiation is the growth of broad (>100 $\text{\AA}$  half width) absorption bands. Figure 6 shows the features observed and Table 1 lists the wavelengths of the maxima of the peaks. The most striking feature is the similarity of all the spectra (except Am). The wavelength of the most intense curium absorption shifts towards the red as the radiation dosage is increased. Only one band was observed for U<sup>3+</sup>-CaF<sub>2</sub> and its wavelength could only be estimated because of the superposition of intense U<sup>3+</sup> absorptions. The band in U is considerably less intense than in the other actinides which might explain the absence of absorptions at  $\sim$ 8000 $\text{\AA}$  and 1.05 $\mu$ . Similar results are obtained for irradiation at 77 $^{\circ}$ K except the intensities are less for comparable dosages. The Np, Pu, and Cm absorption intensities are reduced by approximately factors of ten, three, and two, respectively, relative to the room temperature intensities. We believe these broad bands are due to color centers resulting from the capture of electrons at various defect sites. No report of this particular group of color centers appears in the literature; however these bands are probably related to other observed absorptions in additively colored CaF<sub>2</sub>.<sup>18,19</sup> This interpretation is consistent with the results of the Am-CaF<sub>2</sub> crystal which did not show this type of spectrum but appeared to resemble more closely the behavior of a lanthanide ion. Irradiation of Pu-CaF<sub>2</sub> and Cm-CaF<sub>2</sub> at 77 $^{\circ}$ K produced an additional broad absorption band at approximately

3000 Å (U and Np were totally opaque in this region). This band could be partially bleached out by warming the crystal to 300°K and totally bleached out by heating to ~400°C. A similar band has been observed in all of the lanthanide elements in CaF<sub>2</sub> upon irradiation at 77°K and has been assigned to trapped holes.<sup>5</sup>

#### THERMOLUMINESCENCE

One technique for determining the types of traps formed in radiation damaged crystals is thermoluminescence.<sup>5</sup> We have obtained glow curves for our actinide - CaF<sub>2</sub> crystals (irradiation times at 77°K of up to one hour) in the temperature range 100°K-300°K. Typical results are shown in Fig. 7. In addition to the actinides, the glow curves for the lanthanides Er, Ho, and Tm were run for comparison purposes. The Er, Ho, Tm, Am, and Cm emissions were extremely intense; the Np, Pu, and undoped CaF<sub>2</sub> emissions were very weak and in order to obtain the data the photomultiplier was cooled. The peak temperatures of the glow curves are listed in Table 2. Although the relative intensities differ, and in some cases are missing, all the glow curves are similar. It was not possible to obtain temperature measurements of the weak emission from Np; however even in the case of undoped CaF<sub>2</sub> weak peaks were obtained which may be due to residual impurities. As can be seen from the data the glow peaks appear to be independent of the particular actinide or rare earth ion and therefore we assign these peaks to thermal traps of the host crystals. Our glow peaks in this temperature range are very similar to those of MP which they ascribed to the recombination of a hole with a trapped electron at a cubic lanthanide site.

Rough estimates have been made for the activation energy, E, of the

low temperature glow peaks by two methods. The first method utilized the conventional Arrhenius diagram. The second method for determining activation energies used the equation<sup>20</sup>

$$E = k T_g^2 / (T_2 - T_g)$$

where  $T_g$  is the temperature of the glow peak maximum,  $k$  is the Boltzmann constant, and  $T_2$  is the temperature at half intensity on the high temperature side of the peak. Table 3 lists the results for both methods. These activation energies are approximate, but they show the following trends: similar values of each glow curve are obtained for the different ions and each succeeding glow peak corresponds to a higher activation energy. This confirms the fact that the hole traps formed are independent of the particular lanthanide or actinide ion. Thermoluminescence measurements above room temperature were obtained only for Am and Cm and are shown in Fig. 8. The emission from Pu and Np was too weak to detect. For the high temperature spectra the glow peaks from the two ions appear entirely different which is consistent with different types of traps formed for the room temperature or 0°C irradiations than for the 77°K irradiations.

#### THERMOLUMINESCENCE SPECTRA

We have studied the thermoluminescence spectra of Am and Cm in the temperature range 77°K-300°K and compared them with the spectra obtained from the fluorescence excited by a 1000 watt Hg lamp. It was not possible to obtain similar spectra from Np-CaF<sub>2</sub> and Pu-CaF<sub>2</sub> because of the weak light intensities. The Am thermoluminescence and fluorescence is shown in Fig. 9. Although the thermoluminescence lines are considerably broader than the fluorescence lines it is clear there is one additional line in the fluorescence.

All spectra are assigned to  $\text{Am}^{3+}$  transitions but only a particular site symmetry (probably cubic) is involved in the thermoluminescence. The intense high temperature green emission from  $\text{Am}^{3+}$  at approximately  $500^\circ\text{C}$  has been previously assigned to noncubic sites.<sup>8</sup>

The thermoluminescence ( $77^\circ\text{K}$ - $300^\circ\text{K}$ ) and luminescence ( $77^\circ\text{K}$ ) spectra of  $\text{Cm}^{3+}$ - $\text{CaF}_2$  are shown in Fig. 10. The thermoluminescence spectrum consists of only three sharp lines whose relative splittings are consistent with the ground state splittings found for cubic  $\text{Cm}^{3+}$  ions by electron paramagnetic resonance measurements.<sup>10</sup> However there is no evidence for the excited state splittings which should be quite appreciable. The fluorescence spectrum consists of many more transitions which arise from many other symmetry sites. Thus for  $\text{Cm}^{3+}$ - $\text{CaF}_2$  the thermoluminescence may be assigned to cubic symmetry.

#### DISCUSSION

The data presented in the previous sections may be divided into two parts: the low temperature irradiations ( $77^\circ\text{K}$ ) and processes taking place below room temperature; and  $0^\circ\text{C}$  or room temperature irradiations and high temperature processes. The results may be summarized as follows. At low temperatures:

- (1) the irradiation oxidizes the trivalent actinides but the efficiency is very low at  $77^\circ\text{K}$ ;
- (2) the irradiation produces site symmetry changes for a small number of trivalent actinide ions in particular sites;
- (3) a thermal cycle to room temperature reduces the intensity of the new sites of the trivalent actinide and light emission characteristic of the trivalent

actinide is observed;

(4) the temperatures at which the thermoluminescence occurs is independent of the particular lanthanide or actinide;

(5) the spectrum of the  $Cm^{3+}$  thermoluminescence from 77°K to room temperature is characteristic of a cubic symmetry site;

(6) a color center due to trapped holes appears and may be partially bleached out by warming to 300°K.

(7) the  $Am-CaF_2$  crystals behaves as a typical lanthanide system.

At high temperatures:

(8) irradiation at 0°C or 25°C results in the oxidation of trivalent actinide in particular sites to the tetravalent state (except Am);

(9) color centers are formed at these temperatures which appear to be almost independent of the actinide present as long as that actinide may be oxidized to the tetravalent state;

(10) heating the crystals above room temperature results in thermoluminescence from noncubic sites (for lanthanides and actinides) and the destruction of the color centers and the tetravalent ions of the actinides (except Am).

The results we have obtained are very similar to MP's data for lanthanide ions except for the oxidation of the trivalent actinides. Their low temperature mechanism involved the formation of holes and electrons during the irradiations. Some of the electrons were trapped by trivalent lanthanide ions in cubic sites with resultant reduction. Thermal diffusion of the holes as the temperature increased resulted in the capture of an electron leaving the lanthanide ion in an excited electronic state which subsequently decayed to the ground state with the emission of light. In our 77°K experiments, there appears to be a better electron acceptor than the trivalent actinide ion.



Irradiation produces holes and electrons. A freed electron is attracted by the net +1 charge of a cubic trivalent actinide ion ( $An^{3+}$ ) and is localized near the  $An^{3+}$  ion as to change its site symmetry. As the temperature is raised the hole centers become free to migrate through the crystal until they approach the localized electrons. Recombination occurs with sufficient energy transferred to the nearby  $An^{3+}$  ion to put it in an excited state. The decay of the excited trivalent ion results in the observed cubic thermoluminescence. Different types of trapped holes account for the various glow peaks.

The configuration of the localized electron is not known. The electron could be accepted by a single nearest neighbor  $Ca^{++}$  ion or (as suggested by Weller<sup>21</sup> for  $CdF_2$  crystals) the electron may be shared by the 12 Ca nearest neighbors to the  $An^{3+}$  ion. This allows for a "resonance" stabilized  $Ca^+$  state. Another possibility is that the trapped electron moves in a hydrogenlike orbit about the trivalent actinide impurity.<sup>22</sup>

The room temperature oxidation mechanism was shown previously not to proceed by direct ionization. We suggest instead that irradiation produces fluorine atoms by stripping electrons from interstitial fluoride ions or regular lattice fluorides. One of these fluorine atoms may then diffuse to a nearby  $An^{3+}$  ion and oxidize it by accepting an electron. The electrons trapped in the lattice become free to diffuse through the crystal as the temperature is increased. Recombination with a tetravalent ion leaves an excited trivalent ion which decays to its ground state resulting in the observed emission. Since each electron trap configuration requires a different activation energy to free its electron, several thermoluminescence peaks are observed.

It is apparent from the correlation of the decay of  $Np^{3+}$  with the

growth of  $\text{Np}^{4+}$  that only certain sites with particular charge compensating mechanisms are susceptible to oxidation. Since this mechanism depends on the actual migration of atoms it is very temperature dependent and accounts for the very low yield and site symmetry dependence during  $77^\circ\text{K}$  irradiations. One problem exists with the proposed mechanisms. The new  $\text{Np}^{3+}$  structure is only partially bleached at room temperature after formation at  $77^\circ\text{K}$ . This structure does not appear at room temperature. We suggest the irradiations at room temperature or  $0^\circ\text{C}$  cause the formation of more stable electron traps (better electron acceptors) i.e., fluorine atoms, so that the mechanism suggested for the low temperature irradiations is not favored.

#### CONCLUSION

Spectral changes observed upon gamma irradiation of the actinide ions, U, Np, Pu, and Cm, in  $\text{CaF}_2$  crystals have been divided into two classes, sharp line spectra and broad absorption bands. The new sharp line spectra were assigned to tetravalent ions formed by the oxidation of trivalent ions or to changes in the site symmetry about the trivalent ion. The broad bands were assigned to absorptions from various types of electron or hole traps. Two actinide ions,  $\text{Am}^{3+}$  and  $\text{Es}^{3+}$ , showing behavior analogous to the lanthanide series, were reduced to the dipositive state by irradiation. A mechanism has been proposed to explain the spectral changes and oxidations. Further work is necessary to determine the site symmetries of the trivalent ions which undergo changes, the site symmetries of the tetravalent ions, and the nature of the color centers.

#### ACKNOWLEDGEMENTS

We wish to express our appreciation for the support and encouragement of the late Professor Burris B. Cunningham. We wish to thank J. Conway and H. Mollet for valuable discussions.

FOOTNOTE AND REFERENCES

<sup>†</sup>Work performed under the auspices of the U. S. Atomic Energy Commission.

1. M. J. Weber and R. W. Bierig, Phys. Rev. 134, A1492 (1964).
2. D. S. McClure and Z. J. Kiss, J. Chem. Phys. 39, 3251 (1963).
3. F. K. Fong, J. Chem. Phys. 41, 2291 (1964).
4. Z. J. Kiss and P. N. Yocom, J. Chem. Phys. 41, 1511 (1964).
5. J. L. Merz and P. S. Pershan, Phys. Rev. 162, 217 (1967); *ibid.* 162, 235 (1967).
6. N. Edelstein, W. Easley, and R. McLaughlin, J. Chem. Phys. 44, 3130 (1966).
7. R. McLaughlin, R. White, N. Edelstein, and J. G. Conway, J. Chem. Phys. 48, 967 (1968).
8. N. Edelstein, W. Easley, and R. McLaughlin, Advances in Chemistry Series 71 (American Chemical Society Publications, Washington, D. C., 1967) p.203.
9. N. Edelstein, J. Conway, D. Fujita, W. Kolbe, and R. McLaughlin, J. Chem. Phys. 52, 6425 (1970).
10. N. Edelstein and W. Easley, J. Chem. Phys. 48, 2110 (1968).
11. Optovac, Inc., North Brookfield, Massachusetts.
12. W. F. Krupke and J. B. Gruber, J. Chem. Phys. 46, 542 (1967).
13. W. C. Waggener, J. Phys. Chem. 62, 382 (1958).
14. J. B. Gruber and E. R. Menzel, J. Chem. Phys. 50, 3772 (1970).
15. B. Welber, J. Appl. Physics 36, 2744 (1965).
16. W. A. Hargreaves, Phys. Rev. 156, 331 (1967); Phys. Rev., B2, 2273 (1970).
17. R. McLaughlin, U. Abed, J. G. Conway, N. Edelstein, and E. H. Huffman, J. Chem. Phys. 53, 2031 (1970).
18. F. K. Fong and P. N. Yocum, J. Chem. Phys. 41, 1383 (1964).

REFERENCES (continued)

19. K. S. V. Nambi and T. Higashimura, J. Phys. C4, L134 (1971).
20. A. Halperin and A. A. Branner, Phys. Rev. 117, 408 (1960).
21. P. F. Weller, Inorg. Chem. 4, 1545 (1965).
22. P. Eisenberger and P. S. Pershan, Phys. Rev. 167, 292 (1968).

Table 1. Wavelengths of broad absorptions in  $An^{3+}-CaF_2$ .

U		5500 Å		
Np		5800 Å		1.05 $\mu$
Pu	3800 Å sh	5800 Å	8100 Å	1.07 $\mu$
Cm	3900 Å sh	4800- 5400 Å	7800 Å	1.06 $\mu$

Table 2. Peak temperatures of glow curves (in °K).

Rare Earths	#1	#2	#3	#4	#5
Cm	146		216 sh	241	269
Pu	140	191	215	237	261 sh
Am	140	193		245	
Ho	140	179	205	243	270
Tm	136	177		240	264
Er	141	183	209	246	270
CaF <sub>2</sub>	141	178		243	
Average	140	183	211	242	267
Mean Dev.	±2	±5	±4	±2	±3

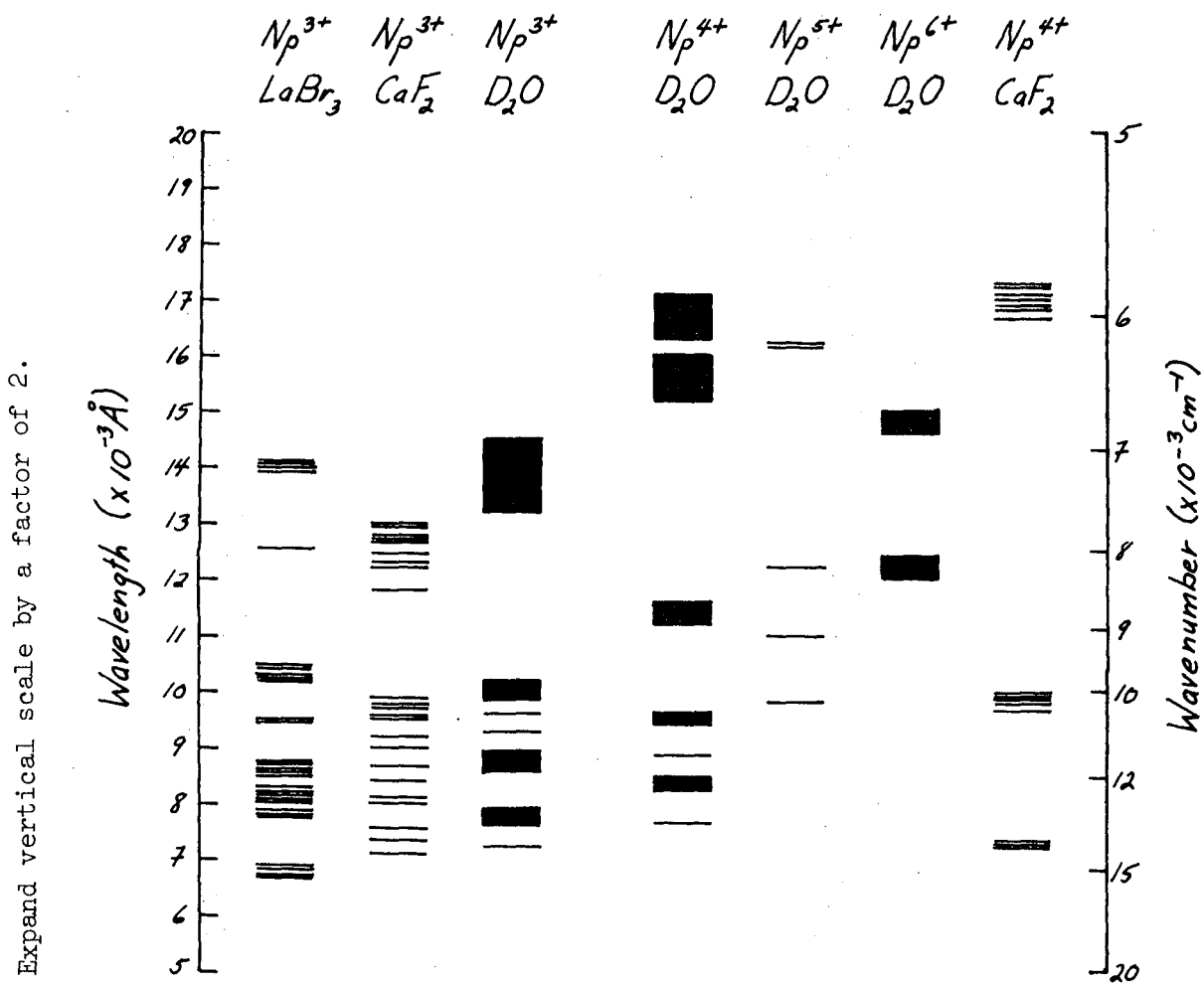
Table 3. Activation energies of rare earth glow peaks. Values obtained using Arrhenius diagrams are not in parentheses; values obtained using the method of Halperin and Braner are in parentheses. (estimated accuracy ~25%).

Rare Earth	#1 E(ev.)	#2 E(ev.)	#3 E(ev.)	#4 E(ev.)	#5 E(ev.)
Cm	.075 (.071)			.44 (.52)	
Pu	.14 (.21)			.47 (.47)	
Am	.24 (.24)	.11 (.29)		.56 (.51)	
Hc					
Tm					
Er	.11 (.25)	.35 (.35)	.47 (.47)	.72 (.72)	.73 (.73)
CaF <sub>2</sub>	.11 (.14)			.65 (.42)	
Average	.11±.02 (.18±.06)	.11 (.32±.03)	.47 (.47)	.53±.08 (.53±.08)	.73 (.73)

FIGURE CAPTIONS

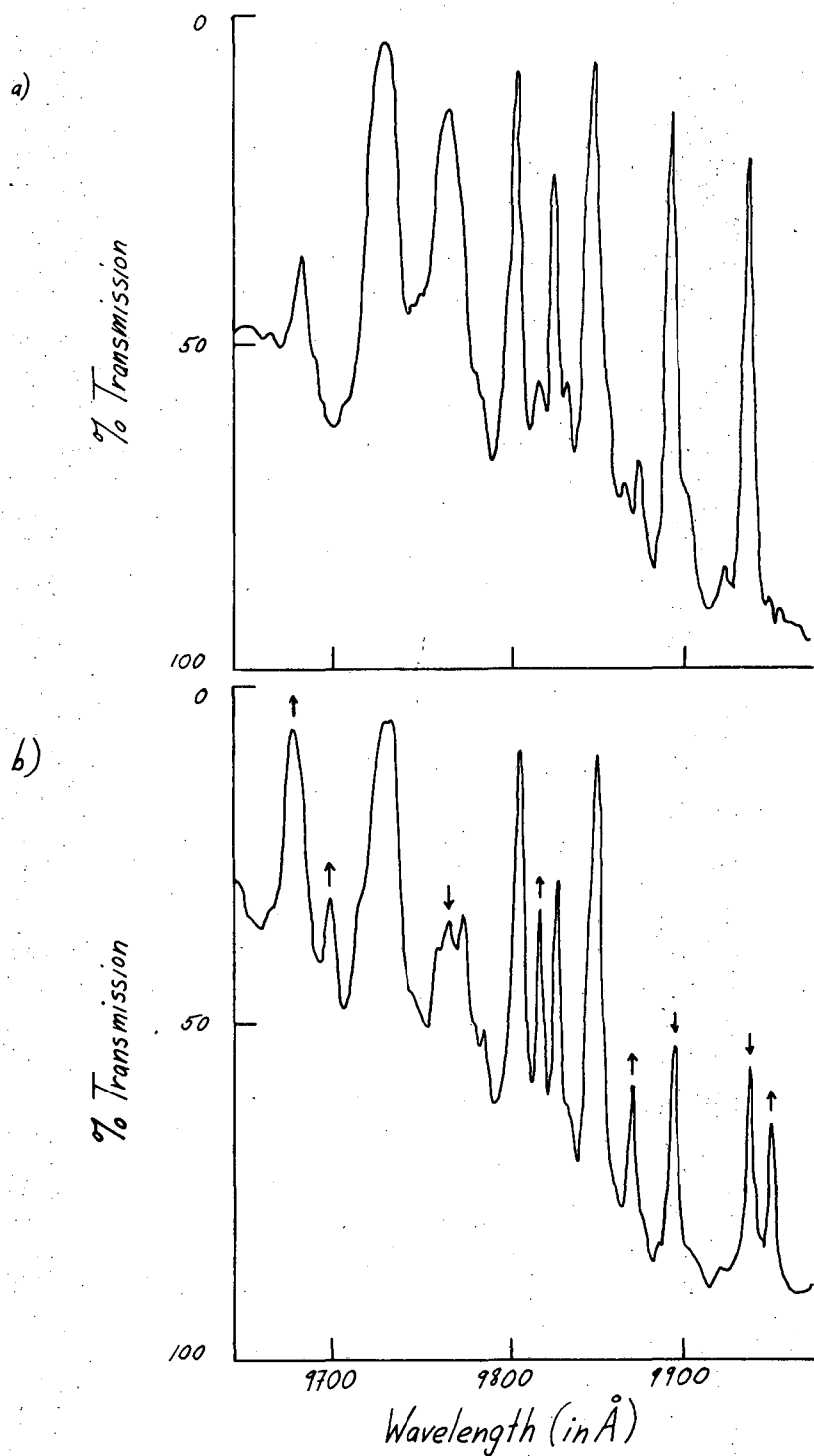
- Fig. 1. Comparison of Np spectra in various media.
- Fig. 2. Absorption spectra of  $\text{Np}^{3+}$ - $\text{CaF}_2$ : a) before irradiation, b) 10 hrs. irradiation at  $0^\circ\text{C}$ . The arrows indicate the absorption lines which increase or decrease upon irradiation.
- Fig. 3. Growth and decay of absorption lines in  $\text{Np-CaF}_2$  as a function of irradiation time.
- Fig. 4. Plot of relative rate of growth of  $\text{Np}^{4+}$  absorption lines versus relative rate of decay of  $\text{Np}^{3+}$  absorption lines.
- Fig. 5.  $\text{Np-CaF}_2$  absorption spectra: a) crystal bleached, b) 48 hrs.  $\gamma$ -irradiation at  $77^\circ\text{K}$ , c) crystal bleached to room temperature. The asterisks denote the new lines formed upon irradiation.
- Fig. 6. Broad absorption spectra of  $\text{Ac}^{3+}$ - $\text{CaF}_2$  after 3 hrs.  $\gamma$ -irradiation. The dotted lines indicate the positions of absorption maxima.
- Fig. 7. Thermoluminescence of  $\text{RE}^{3+}$ - $\text{CaF}_2$ . All irradiations were at  $77^\circ\text{K}$  for 30 minutes in a  $^{60}\text{Co}$  source. The dotted lines indicate the positions of glow peak maxima.
- Fig. 8. a) Thermoluminescence of  $\text{Am-CaF}_2$ . b) Thermoluminescence of  $\text{Cm-CaF}_2$ . The temperature scale is not linear.
- Fig. 9. Densitometer tracings of photographic plates: a) spectrum of the low temperature thermoluminescence of  $\text{Am-CaF}_2$ , b) fluorescence spectrum of  $\text{Am}^{3+}$ - $\text{CaF}_2$  at  $77^\circ\text{K}$ .
- Fig. 10. Densitometer tracings of photographic plates: a) Hg-excited fluorescence of  $\text{Cm}^{3+}$ - $\text{CaF}_2$  at  $77^\circ\text{K}$ , b) spectrum of low temperature thermoluminescence of  $\text{Cm}^2$ - $\text{CaF}_2$ .





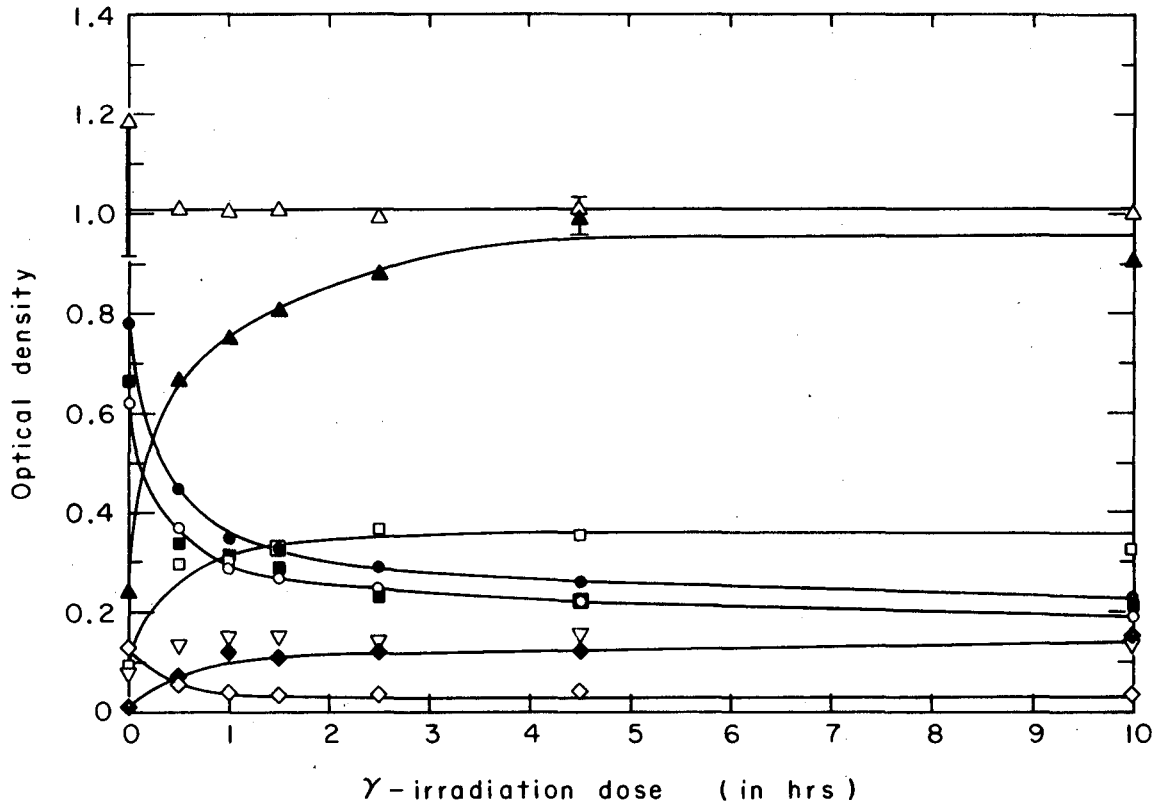
XBL 7141-1673

Fig. 1. Comparison of Np spectra in various media.



XBL 7111-1655

Fig. 2. Absorption spectra of  $\text{Np}^{3+}$ - $\text{CaF}_2$ : a) before irradiation, b) 10 hrs irradiation at 0°C. The arrows indicate the absorption lines which increase or decrease upon irradiation.

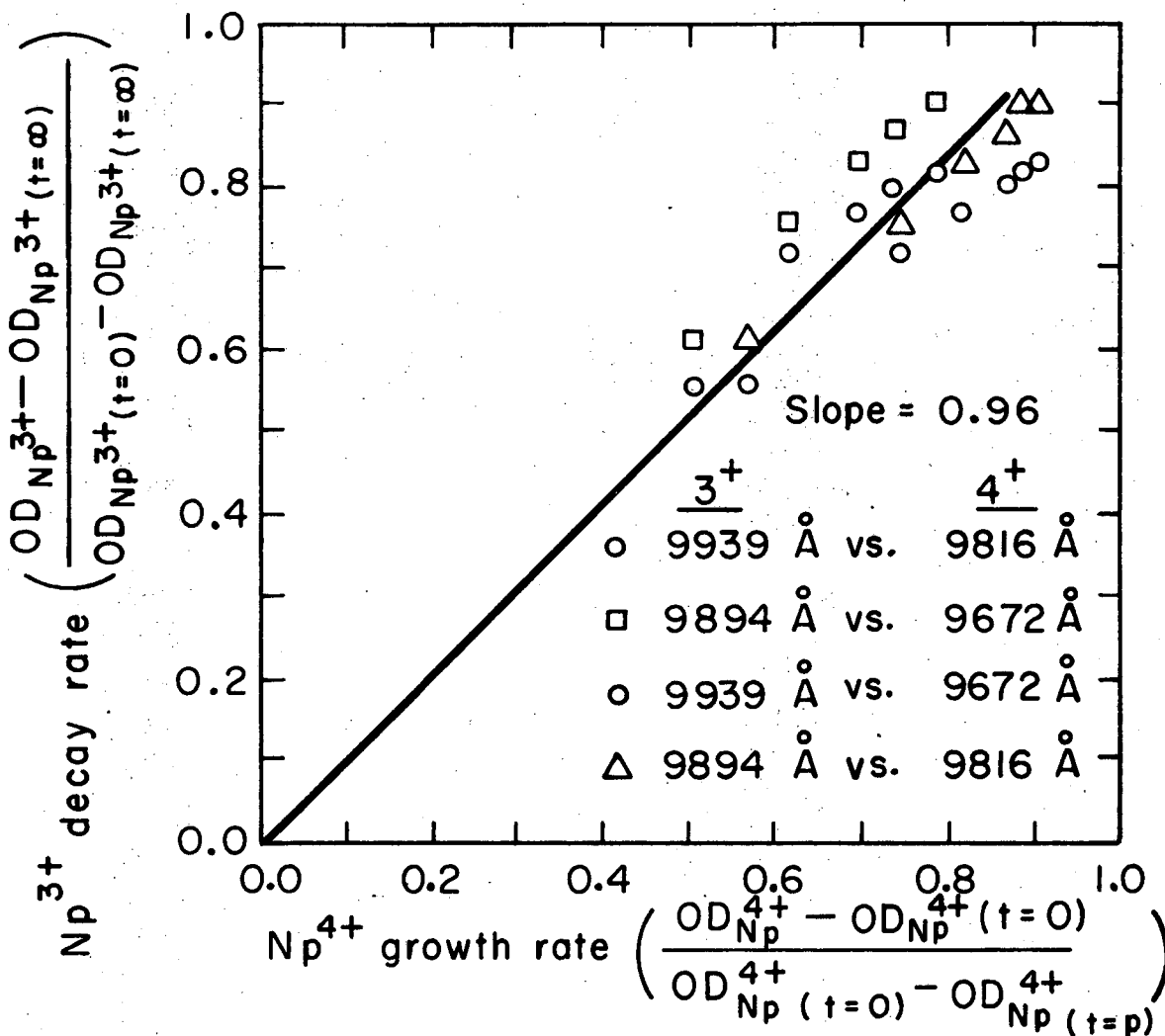


$Np^{4+}$   $Np^{3+}$

▲ 9672 Å	▽ 9870 Å	◇ 9590 Å	■ 9764 Å
□ 9816 Å	◆ 9951 Å	△ 9728 Å	● 9894 Å
		○ 9939 Å	

XBL 7111-1663

Fig. 3. Growth and decay of absorption lines in  $Np-CaF_2$  as a function of irradiation time.



XBL723-2626

Fig. 4. Plot of relative rate of growth of  $\text{Np}^{4+}$  absorption lines versus relative rate of decay of  $\text{Np}^{3+}$  absorption lines.

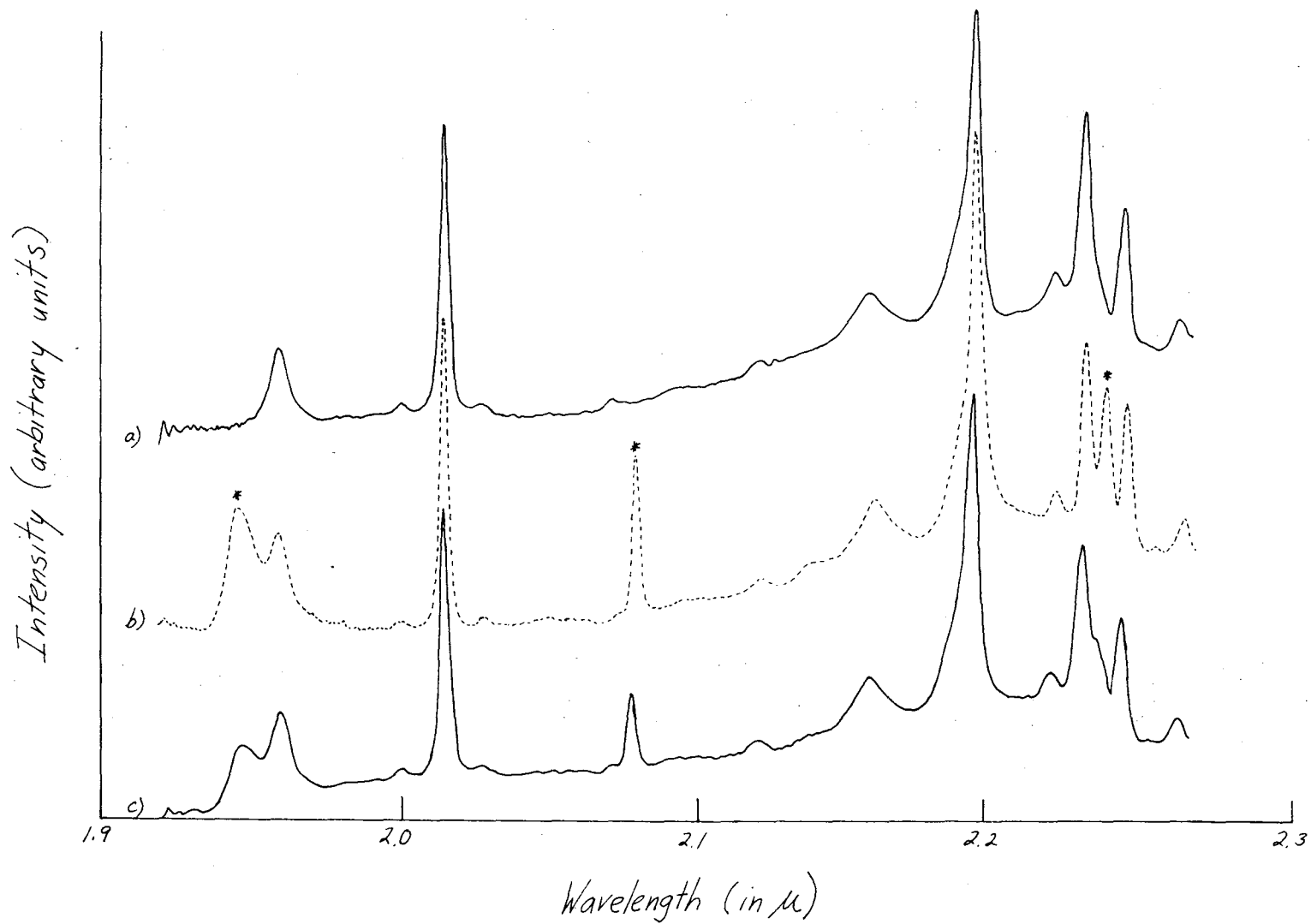
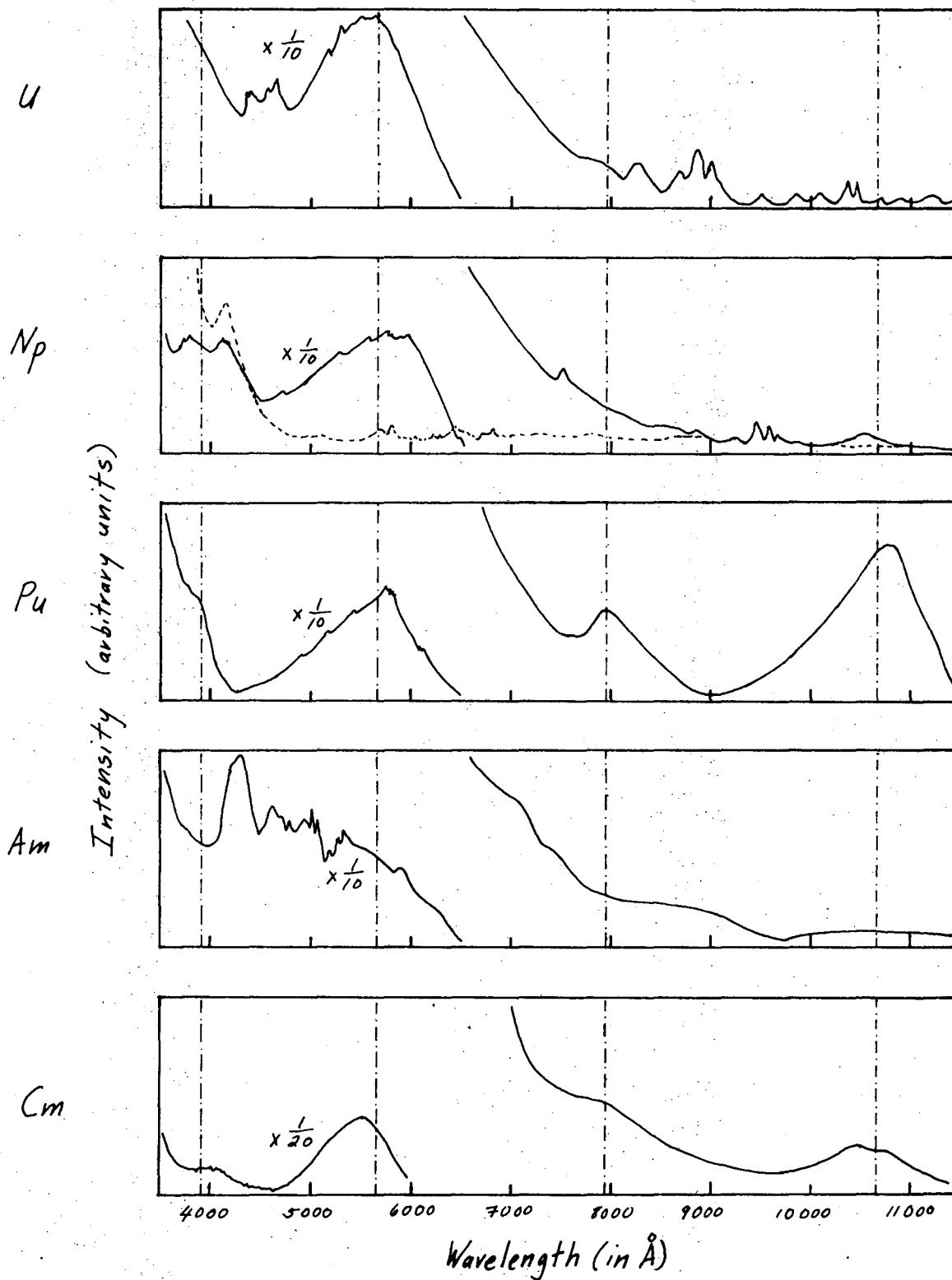


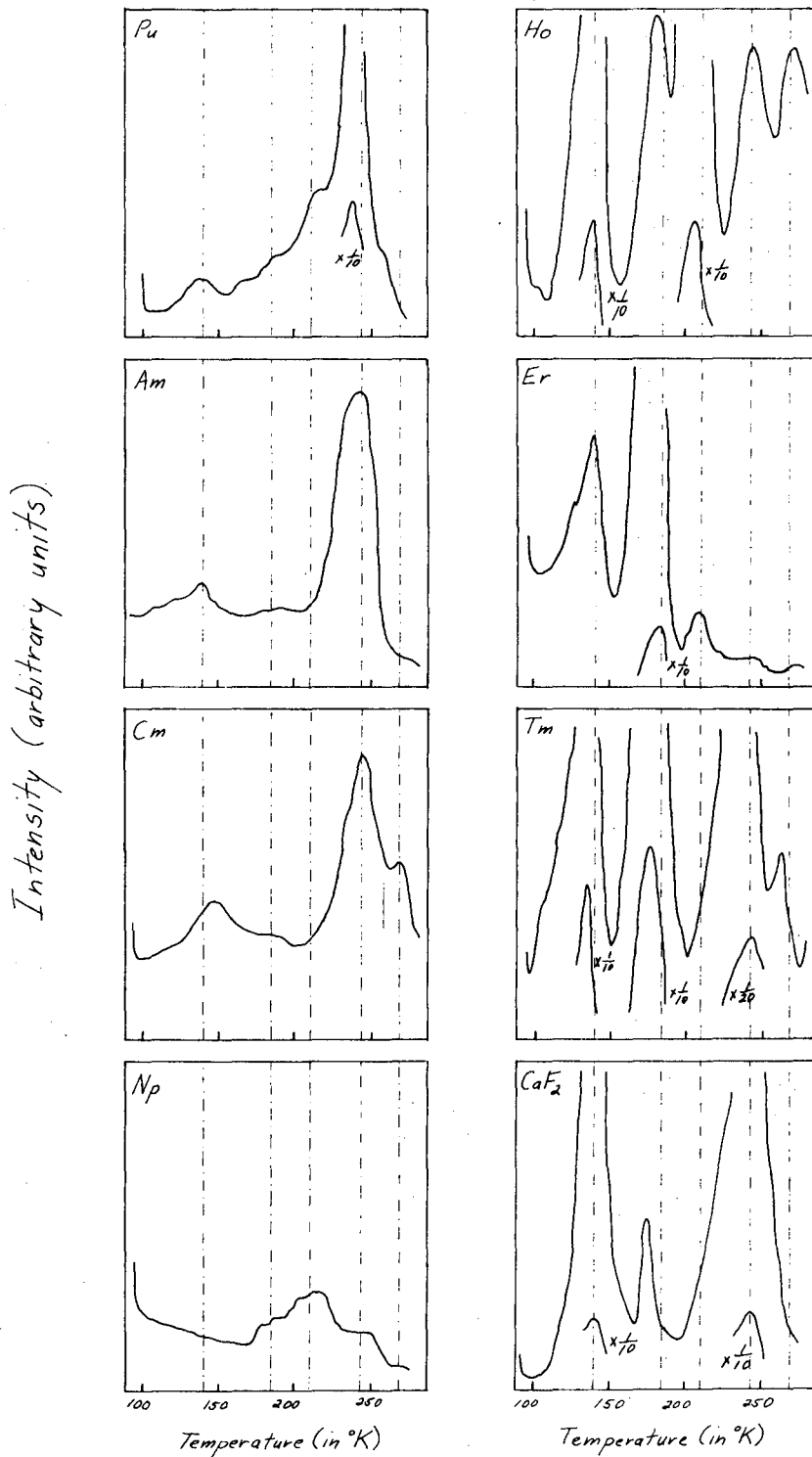
Fig. 5. Np-CaF<sub>2</sub> absorption spectra: a) crystal bleached, b) 48 hrs.  $\gamma$ -irradiation at 77°K, c) crystal bleached to room temperature. The asterisks denote the new lines formed upon irradiation.

XBL 7111-1656



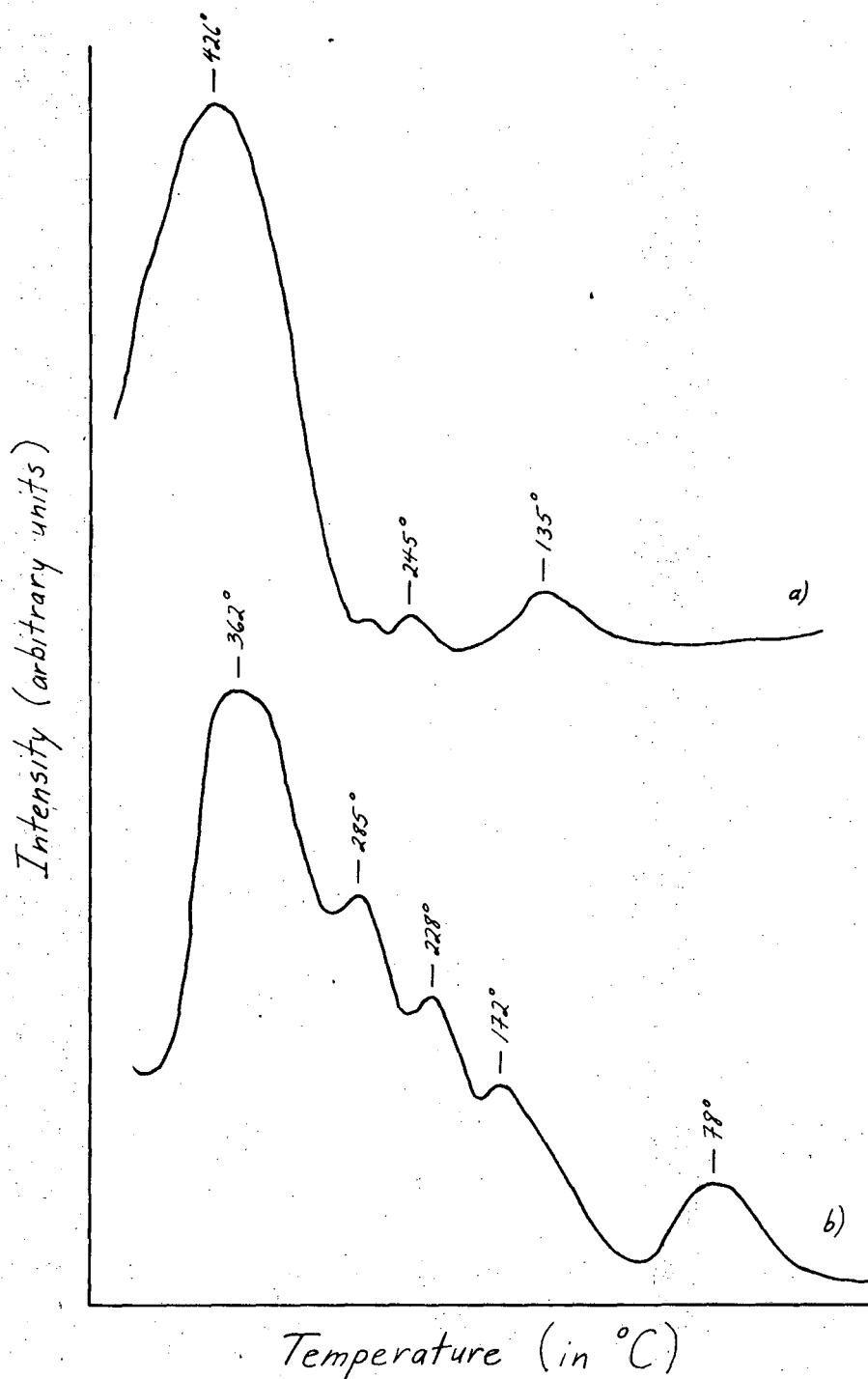
XBL 7111-1682

Fig. 6. Broad absorption spectra of  $\text{Ac}^{3+}\text{-CaF}_2$  after 3 hrs.  $\gamma$ -irradiation. The dotted lines indicate the positions of absorption maxima.



XBL 7111-1657

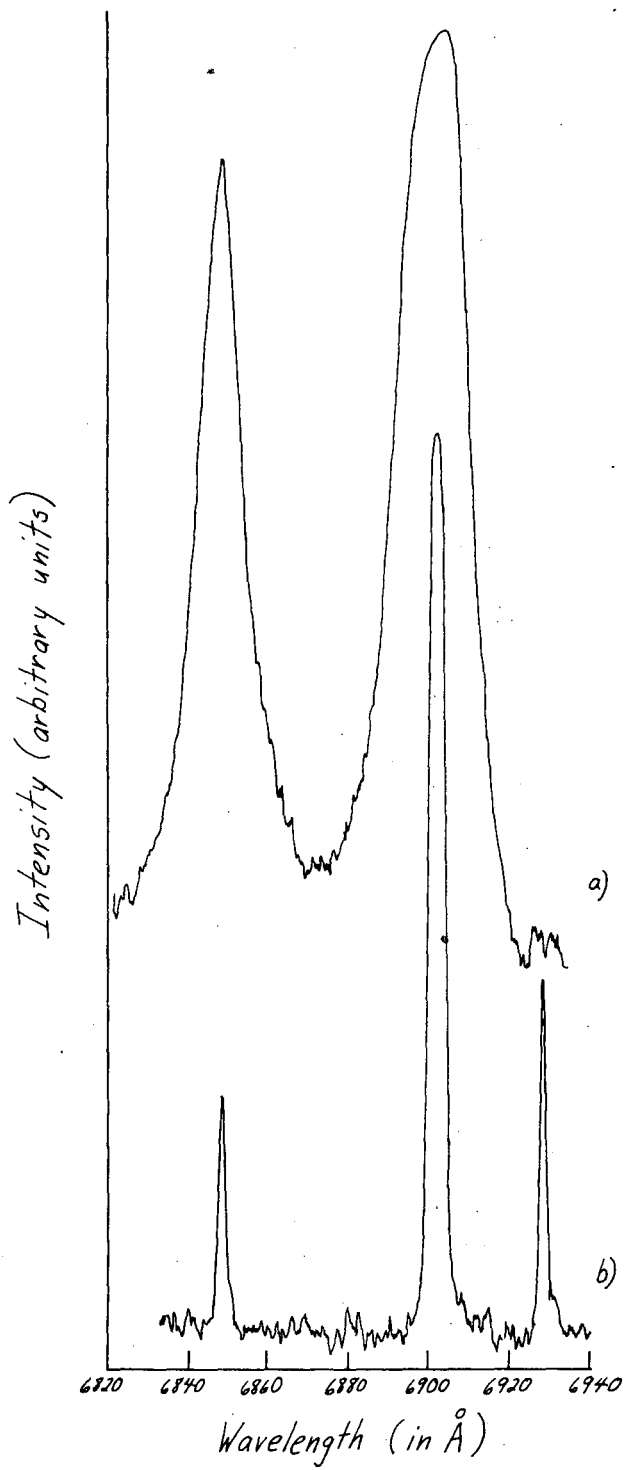
Fig. 7. Thermoluminescence of RE<sup>3+</sup>-CaF<sub>2</sub>. All irradiations were at 77°K for 30 minutes in a <sup>60</sup>Co source. The dotted lines indicate the positions of glow peak maxima.



XBL 7111-1660

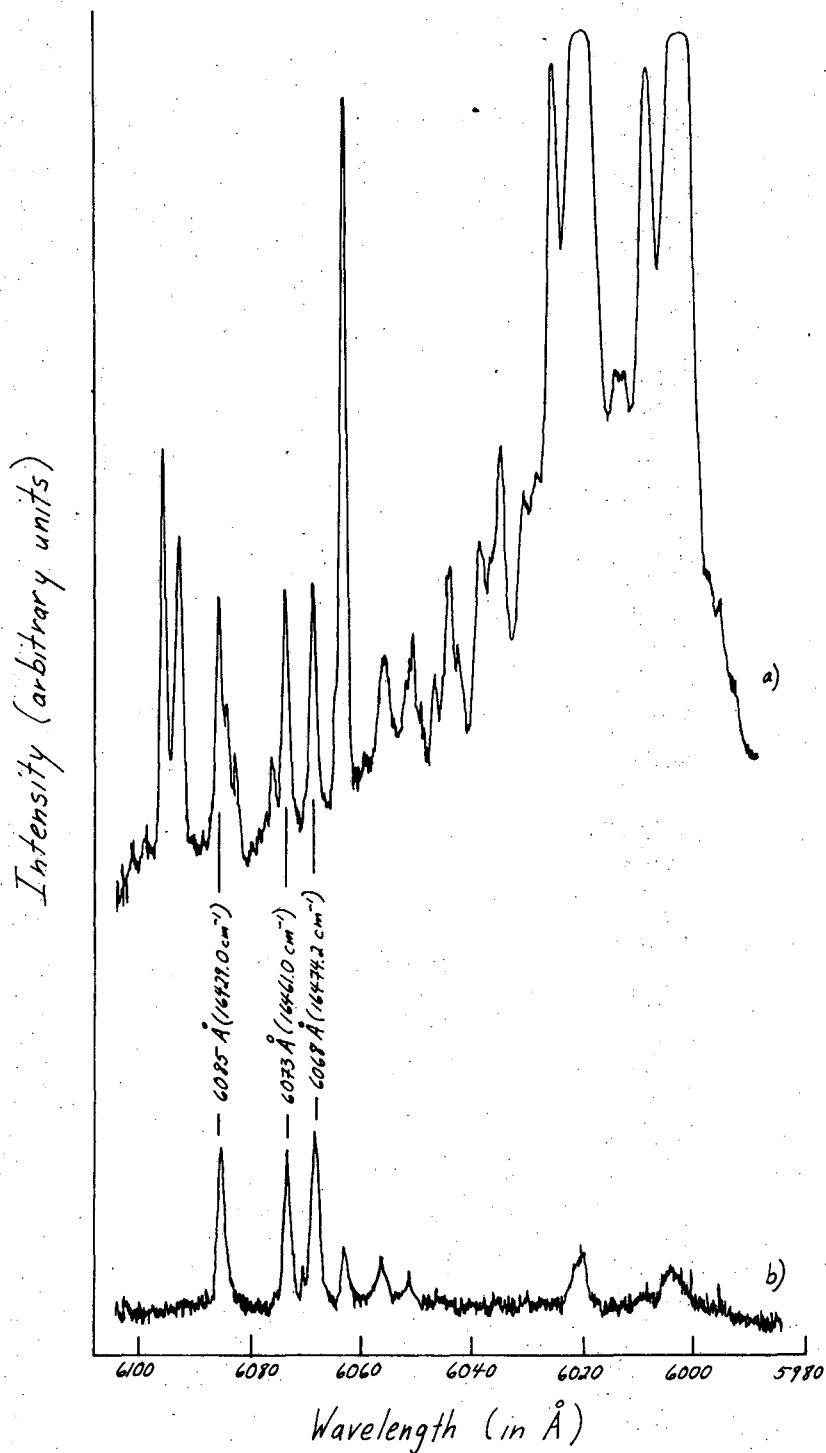
Fig. 8. a) Thermoluminescence of Am-CaF<sub>2</sub>. b) Thermoluminescence of Cm-CaF<sub>2</sub>. The temperature scale is not linear.





XBL 7111-1659

Fig. 9. Densitometer tracings of photographic plates: a) spectrum of the low temperature thermoluminescence of Am-CaF<sub>2</sub>, b) fluorescence spectrum of Am<sup>3+</sup>-CaF<sub>2</sub> at 77°K.



XBL 7111-1661

Fig. 10. Densitometer tracings of photographic plates: a) Hg-excited fluorescence of Cm<sup>3+</sup>-CaF<sub>2</sub> at 77°K, b) spectrum of low temperature thermoluminescence of Cm-CaF<sub>2</sub>.

LEGAL NOTICE

*This report was prepared as an account of work sponsored by the United States Government. Neither the United States nor the United States Atomic Energy Commission, nor any of their employees, nor any of their contractors, subcontractors, or their employees, makes any warranty, express or implied, or assumes any legal liability or responsibility for the accuracy, completeness or usefulness of any information, apparatus, product or process disclosed, or represents that its use would not infringe privately owned rights.*

TECHNICAL INFORMATION DIVISION  
LAWRENCE BERKELEY LABORATORY  
UNIVERSITY OF CALIFORNIA  
BERKELEY, CALIFORNIA 94720